Solid state stabilisation of the orally delivered drugs atenolol, glibenclamide, memantine and paracetamol through their complexation with cucurbit[7]uril†

Fiona J. McInnes,[a] Nahoum G. Anthony,[a] Alan R. Kennedy[b] and Nial J. Wheate*[a]

Received 8th September 2009, Accepted 20th November 2009
First published as an Advance Article on the web 4th January 2010
DOI: 10.1039/b918372h

The inclusion of the cardiovascular β-blocker drug atenolol, the antidiabetic drug glibenclamide, the Alzheimer's NMDA glutamate receptor drug memantine and the analgesic/antipyretic drug paracetamol by cucurbit[7]uril (CB[7]) has been studied by ^{1}H nuclear magnetic resonance spectroscopy, electrospray ionisation mass spectrometry, molecular modelling, fluorescence displacement assays and differential scanning calorimetry. All four drugs form 1 : 1 host–guest complexes with CB[7], but the exchange kinetics and location of the binding is different for each drug. Atenolol is bound over the central phenyl ring with a binding constant of 4.2×10^4 M^{-1}, whereas glibenclamide is bound over the terminal cyclohexyl group with a binding constant of 1.7×10^5 M^{-1}, and memantine is totally bound within the CB[7] cavity. Paracetamol is bound in two locations, over the central phenyl ring and over the methyl group, with the CB[7] molecule shuttling quickly between the two sites. Inclusion by CB[7] was shown by differential scanning calorimetry to physically stabilise all four drugs, which has applications preventing drug degradation and improving drug processing and formulation.

1. Introduction

The development of novel drug delivery systems for already approved drugs is cheaper ($20–50 million) and less time consuming (3–4 years), than the development of new drugs (~$500 million and 10–12 years).[1] New drug delivery vehicles, which can make current drugs more water soluble, more resistant to degradation in storage or *in vivo*, simplify or make production cheaper, improve their rate of absorption or alter their distribution in the body, mask poor taste or act as controlled release systems, are of considerable interest. Additionally, the use of drug delivery vehicles allows for the attachment of targeting agents, such as aptamers,[2] monoclonal antibodies or peptides,[3] or substrates like folate,[4] which can further improve their efficacy and reduce their side-effects.

The most efficient way to administer drugs in humans is through oral delivery using tablets, capsules or powders, as this method has fewer aseptic constraints, is more flexible in the design of the dosage form and has better patient compliance than injections or liquid oral formulations.[1,5] Therefore, the development of delivery vehicles that are able to encapsulate orally active drugs are of particular interest.

Cucurbit[*n*]urils (CB[*n*]; where $n = 5$, 6, 7, 8 or 10) are a family of macrocycles made from the condensation reaction of glycoluril and formaldehyde in acid (Fig. 1).[6,7] Their hydrophobic cavity and hydrophilic portals allow the macrocycles to form a range of host–guest complexes with organic and inorganic compounds, and noble gases.[8–17] These host–guest complexes can be analysed in the aqueous phase using a range of techniques, including one- and two-dimensional NMR,[8,18] diffusion NMR,[19] electrospray ionisation or MALDI mass spectrometry,[20,21] and UV-Vis or fluorescence spectrophotometry.[22–24]

Through the formation of host–guest complexes, CB[*n*]s, particularly CB[7], can be used for controlled drug delivery.[25,26] Previously, we have examined their use for the delivery of platinum-based anticancer drugs[27] and the antibiotic proflavine.[28] Others have also examined the host–guest complexes of CB[*n*]s with other biologically relevant molecules like vitamin B_{12}[29] and organic drugs[14,30–35] like albendazole. CB[6], CB[7] and CB[8] are similar in size and shape to α-, β- and γ-cyclodextrins, which are cyclic oligosaccharides composed of α-D-glucose units joined by α-1,4-linkages.[36–38] With their hydrophobic internal cavity, cyclodextrins are able to form non-covalent inclusion complexes with a variety of compounds, and as such, are already used as drug delivery vehicles in a number of approved formulations.[36–38]

As well as drug delivery vehicles, CB[*n*]s may also serve a double purpose by stabilising drugs during manufacture. Recently, we have examined the processing and formulation of cucurbit[*n*]urils, using CB[6] as a model compound, as excipients in oral tablet formulations.[39] Pure CB[6] can not be compressed into tablets, but when combined with a mixture of typical excipients such as talc, magnesium stearate, lactose, Avicel® and Ac-Di-Sol®, tablets containing up to 40% w/w CB[6] can be produced. These tablets display good pharmaceutical properties with acceptable tablet hardness, and disintegration and dissolution times.[39] The next step in the development of CB[*n*]s as oral drug delivery vehicles is the processing and formulation of CB[*n*]–drug host–guest complexes into tablets, and it is therefore necessary to examine the interaction of several orally delivered drugs with CB[*n*]s.

[a]*Strathclyde Institute of Pharmacy and Biomedical Sciences, University of Strathclyde, John Arbuthnott Building, 27 Taylor Street, Glasgow, United Kingdom G4 0NR. E-mail: nial.wheate@strath.ac.uk; Fax: +44 141 552 2562; Tel: +44 141 548 4962*
[b]*Department of Pure and Applied Chemistry, University of Strathclyde, Royal College Building, 204 George Street, Glasgow, United Kingdom G1 1XW*

† Electronic supplementary information (ESI) available: A video showing the interaction of paracetamol with cucurbit[7]uril. CCDC reference number 746893. For ESI and crystallographic data in CIF or other electronic format see DOI: 10.1039/b918372h

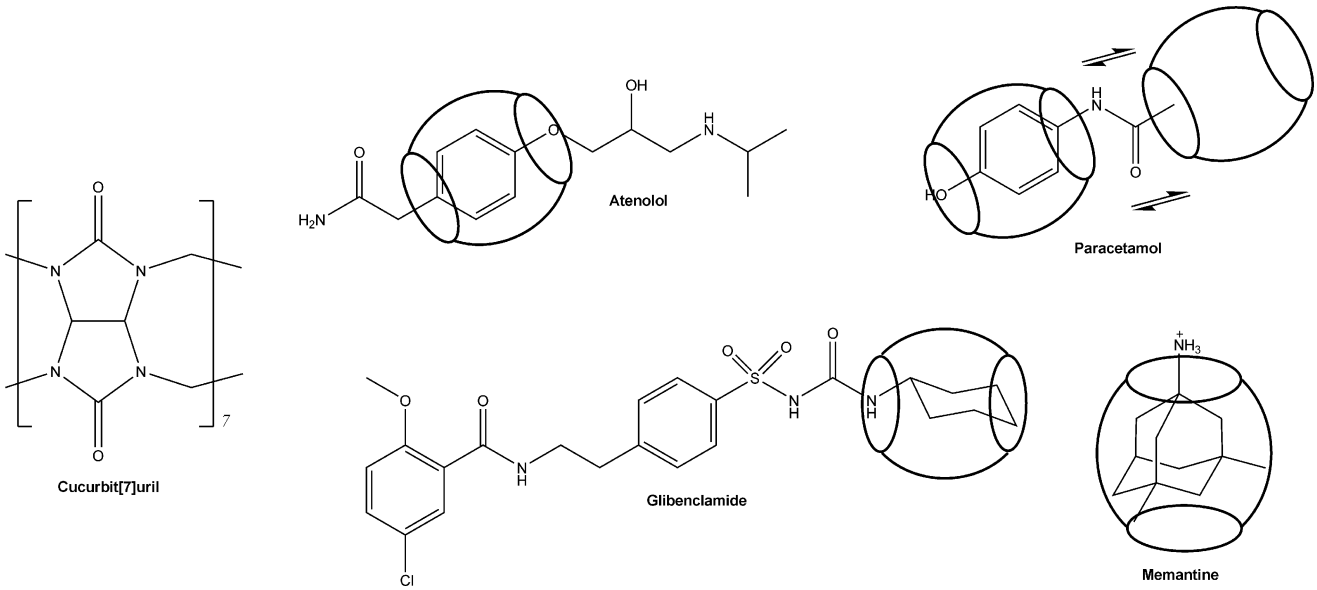

Fig. 1 The chemical structures of the organic drugs and cucurbit[7]uril used in this study, showing the proposed macrocycle binding sites.

In this paper, we examined the host–guest chemistry of four orally delivered drugs used in the treatment of human disease: atenolol, a cardiovascular β-blocker; glibenclamide, an antidiabetic drug; memantine, an Alzheimer's NMDA glutamate receptor drug; and paracetamol, an analgesic/antipyretic drug (see Fig. 1), with CB[7] prior to their formulation into tablets. These drugs represent a range of molecules with different properties: long/short, charged/uncharged, water soluble/insoluble, single/multiple CB[*n*] binding sites, from which the general potential of CB[*n*]s as drug delivery vehicles can be evaluated. CB[7] was chosen, as the cavities of CB[5] and CB[6] are too small to allow the encapsulation of most drugs. In addition, both CB[6] and CB[8] are very poorly soluble in water, and as such, have limited potential as drug delivery vehicles. The drug–CB[7] host–guest complexes were analysed by ^{1}H nuclear magnetic resonance, electrospray ionisation mass spectrometry, molecular modelling, fluorescence displacement assays and differential scanning calorimetry, and the results are discussed in a pharmaceutical and drug delivery context.

2. Results and discussion

2.1 ^{1}H NMR

The inclusion of the four organic drugs atenolol, glibenclamide, memantine and paracetamol by CB[7] was studied by ^{1}H NMR at various drug : CB[7] ratios. In all cases, drug inclusion by CB[7] is observed through large upfield shifts of selected drug proton resonances.

2.2.1. Atenolol. For atenolol in an excess of CB[7], the largest changes are observed for the two phenyl resonances at 7.22 and 6.97 ppm, which move upfield by 0.73 and 0.88 ppm, respectively (Fig. 2). A relatively small upfield shift (0.17 ppm) of the neighbouring methylene resonance is also observed, among other changes in the remaining peaks. These chemical shift changes indicate that atenolol is partially bound by CB[7], with binding

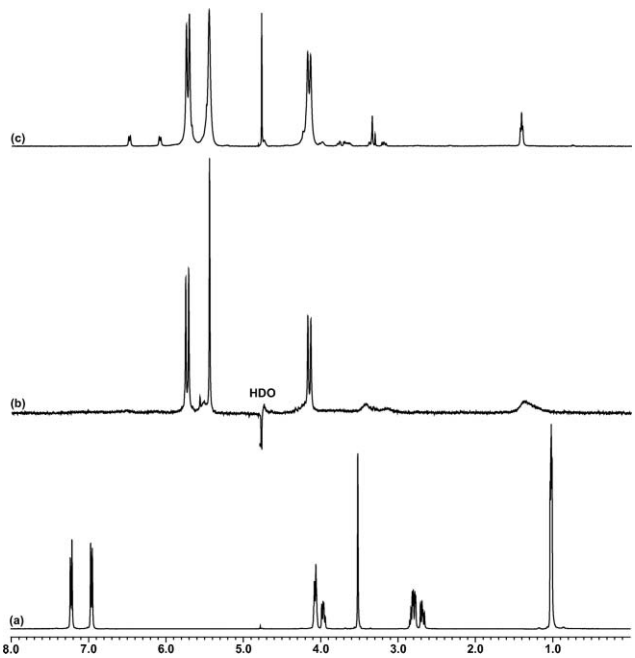

Fig. 2 The ^{1}H NMR spectra (D_2O) of (a) free atenolol, (b) atenolol and CB[7] at a ratio of 2 : 1 and (c) atenolol with excess CB[7]. The large upfield shifts of the aromatic resonances indicate that atenolol is bound over the phenyl ring; see Fig. 7 for the proposed structure.

largely located over the phenyl ring of the drug. When CB[7] is added to atenolol at a drug : CB[7] ratio of 2 : 1, only one set of considerably broadened drug resonances is observed indicating that the binding kinetics are fast to intermediate on the NMR time scale.

2.1.2. Glibenclamide. Glibenclamide is insoluble in water, so the NMR spectrum of the free drug was determined in D_2O/d_6-DMSO (Fig. 3). In this solvent, glibenclamide displays 17 resonances in addition to the solvent peak at 1.66 ppm and the

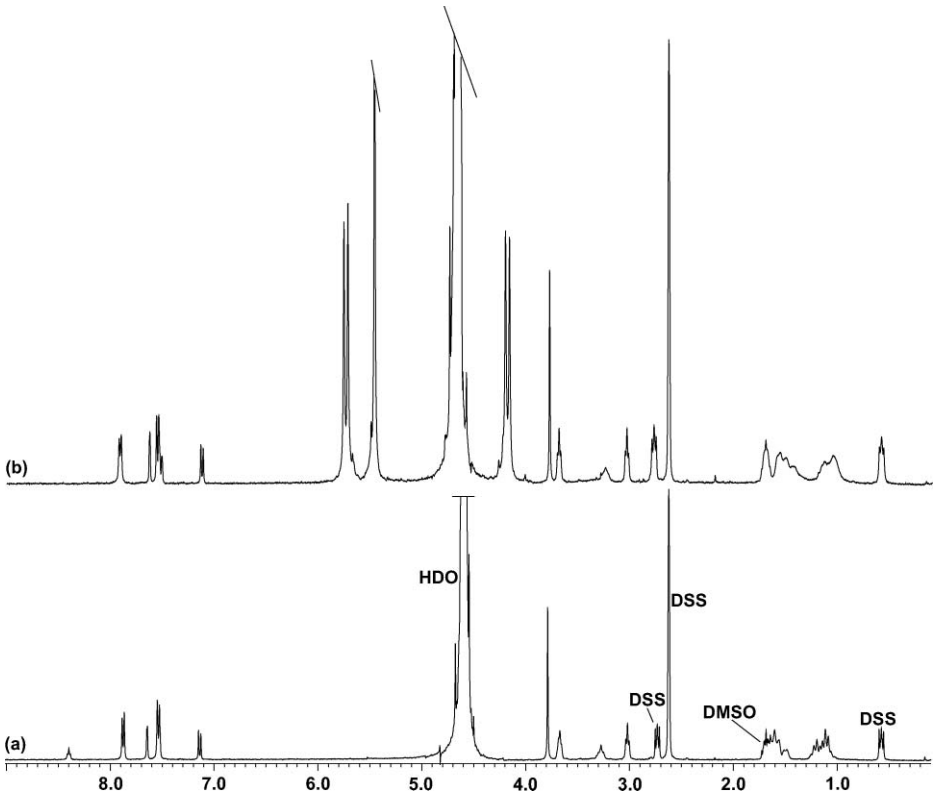

Fig. 3 The ^{1}H NMR spectra (50% D_2O–50% DMSO) of (a) free glibenclamide and (b) glibenclamide with CB[7]. The change in the chemical shift and line broadening of the cyclohexane resonances between 1 and 1.6 ppm, compared with the other drug resonances, indicates that CB[7] binds over this end of the drug; see Fig. 7 for the proposed structure.

DSS peaks at 2.72, 2.61, 0.56 and 0.0 ppm. The resonances of the cyclohexyl protons are well-separated as a group of peaks between 1.0 and 1.6 ppm. In d_6-DMSO 50%–D_2O 50% solutions and at a concentration of 1 mM glibenclamide and CB[7], a large amount of white precipitate is observed, although a sufficient quantity of glibenclamide dissolves so that a spectrum can be obtained. Under these conditions, and by integration of the CB[7] methine and the drug methyl resonances, there is an excess of CB[7] dissolved in solution compared to glibenclamide, which suggests that the majority of the precipitate is free drug and that any glibenclamide in solution is bound by CB[7]. When bound by CB[7], upfield shifts and a general broadening of the glibenclamide cyclohexyl resonances are observed compared with the other drug resonances. This result implies that the CB[7] encapsulates one end of the drug, although solvent effects cannot be discounted.

2.1.3 Memantine. Inclusion of memantine, and its derivatives, by CB[7] and CB[8] has previously been examined by Liu *et al.*[31] Whilst a binding constant of 2.50 (±0.39) × 10^4 M^{-1} and a binding model are reported, no NMR or kinetic exchange data was reported.

Free memantine has only six apparent proton resonances, due to peak overlap, in the ^{1}H NMR aliphatic region between 0.8 and 2.2 ppm. Upon addition of an excess of CB[7], all the drug resonances shift upfield and split into eight discernable peaks with chemical shifts between 0.2 and 1.7 ppm (Fig. 4). Most notably, the memantine methyl resonance moves from 1.34 to 0.43 ppm. The fact that all the drug resonances move upfield indicates that the drug is almost entirely enclosed within the CB[7] cavity, with just the charged memantine NH_3 group sitting beyond the CB[7] portals. At a memantine : CB[7] ratio of 2 : 1, two sets of memantine peaks are observed, representing free and bound drug. This indicates slow binding kinetics on the ^{1}H NMR timescale.

2.1.4 Paracetamol. Finally, the ^{1}H NMR spectrum of free paracetamol has just three non-exchangeable proton resonances in D_2O: two doublet resonances at 7.18 and 6.86 ppm for the phenyl protons, and a singlet resonance at 2.09 ppm for the methyl protons (Fig. 5). Regardless of the paracetamol : CB[7] ratio (either 0.5 : 1, 1 : 1 or 2 : 1), two sets of paracetamol drug peaks are always observed, indicating that CB[7] binds over two separate locations on the drug simultaneously. If the two sets of peaks simply represented free and bound forms of the drug, it would be expected that the spectrum may change over time as the solution comes to equilibrium. If binding is based on very slow inclusion kinetics, this means it would be expected that the peaks for "bound" drug would increase and the peaks for "free" drug would decrease upon the addition of more CB[7]. Given that the NMR spectrum does not change upon storage of the sample for prolonged periods (up to 7 days) and the ratio of the two sets of drug peaks does not change upon addition of more CB[7] over this time period, these results are consistent with CB[7] binding over two different binding sites on paracetamol.

For one set of peaks (△), only the methyl resonance has moved upfield by 0.66 ppm to 1.43 ppm, whilst the phenyl resonances remain unchanged. In the other set of peaks (○), only the phenyl

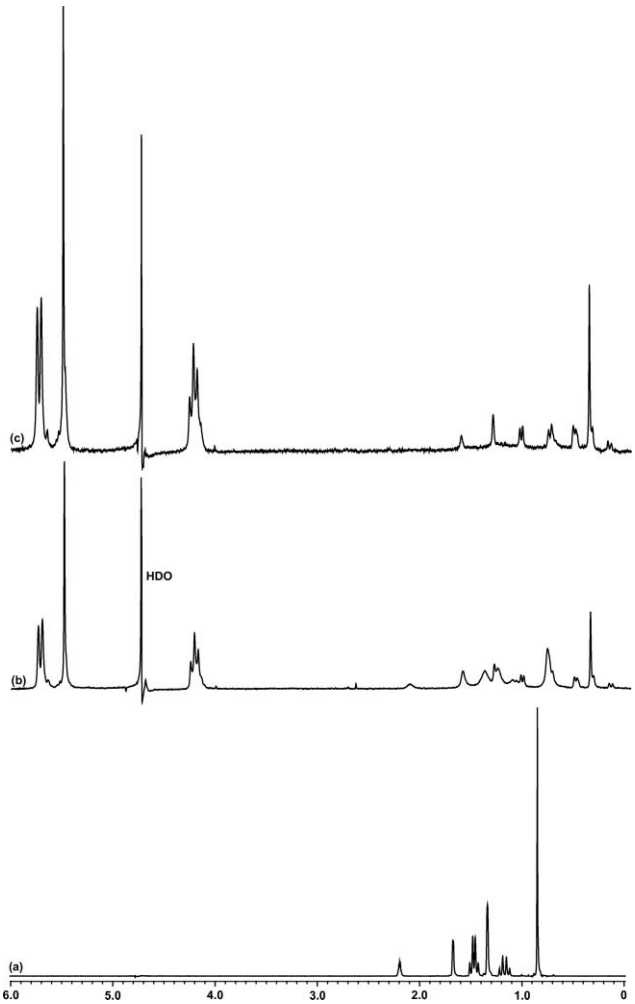

Fig. 4 The ^{1}H NMR spectra (D_2O) of (a) free memantine, (b) memantine and CB[7] at a ratio of 2 : 1, and (c) memantine with excess CB[7].

protons have shifted upfield, in this case by 0.97 and 0.83 ppm, to 6.21 and 6.02 ppm, respectively, and the methyl peak remains relatively unchanged. Interestingly, the addition of CB[7] also allows the observation of the amide proton resonance in pure D_2O, even after prolonged standing, which is seen as a broad shoulder on the CB[7] methine peak at 5.48 ppm. This NH resonance is present even when the drug : CB[7] ratio is 2 : 1, which suggests that the amide proton is protected from solvent exchange due to the rapid shuttling of the CB[7] molecule between the two binding locations on paracetamol.

Taken together, the ^{1}H NMR results for these four drugs, which represent a wide variety of structures including: long/short, charged/uncharged, water soluble/insoluble, single/multiple CB[*n*] binding sites, allow a general assessment of CB[7] as drug delivery vehicles for further organic drugs. Potentially any drug molecule, whether small or large, as long as it has one section within its structure that is a hydrophobic straight chain or *para*-substituted phenyl or benzyl ring to which the CB[7] can bind inside its cavity, can form host–guest complexes with CB[7]. This could include small or large organic drugs, inorganic drugs with organic ligands or peptide-based drugs with suitable and accessible amino acid side chains, like lysine or arginine. However, not all drugs, regardless of their ability to fit inside the cavity of CB[7], will form host–guest complexes. For instance, as part of this study we investigated the attempted inclusion of the non-steroidal anti-inflammatory drug ibuprofen, 2-(4-isobutylphenyl)propanoic acid, within CB[7], which subsequently was found not to form host–guest complexes with the macrocycle. Whilst it does contain several potential hydrophobic binding sites for inclusion within the CB[7] cavity, it lacks a group capable of forming hydrogen bonds to the CB[7] portals. Therefore, it appears to be preferable for drugs to contain either a positive charge or an am(mine)/amide group in order to further stabilise drug–CB[7] host–guest binding.

Table 1 The electrospray ionisation mass spectrometry calculated and observed peaks of the host–guest complexes of atenolol, glibenclamide, memantine and paracetamol with cucurbit[7]uril

Drug	Host–guest complex	Calc' (*m*/*z*)	Observed (*m*/*z*)
Atenolol	$[Drug + CB7 + H^+ + Na^+]^{2+}$	726.2	726.5
Atenolol	$[Drug + CB7 + 2H^+]^{2+}$	715.2	715.5
Atenolol	$[Drug + CB7 + H^+]^+$	1429.4	1429.6
Glibenclamide	$[Drug + CB7 + H^+ + Na^+]^{2+}$	839.8	840.2
Glibenclamide	$[Drug + CB7 + 2Na^+]^{2+}$	849.8	850.9
Glibenclamide	$[Drug + CB7 + Na^+]^+$	1678.5	1678.3
Memantine	$[Drug + CB7 + H^+]^+$	1342.5	1343.6
Paracetamol	$[Drug + CB7 + H^+ + Na^+]^{2+}$	668.7	669.9
Paracetamol	$[Drug + CB7 + 2Na^+]^{2+}$	679.7	680.3
Paracetamol	$[Drug + CB7 + H^+]^+$	1314.4	1315.4

2.2 Mass spectrometry

The interaction of the four drugs with CB[7] was further examined using electrospray ionisation mass spectrometry. In all cases, peaks corresponding to free drug and free CB[7] were observed (CB[7] + $2H^+$, 582 *m*/*z*; CB[7] + H^+ + Na^+, 593 *m*/*z*, CB[7] + H^+, 1163 *m*/*z*; CB[7] + Na^+, 1185 *m*/*z*; CB[7] + K^+, 1202 *m*/*z*). Host–guest complex peaks are also observed for each drug as a range of 1+ and 2+ species (Table 1). For all four drugs, 1 : 1 host–guest complexes are observed. There are no peaks that indicate the formation of 2 : 1 drug : CB[7] host–guest complexes, nor is any peak observed for paracetamol with two CB[7] molecules, as would be the case if the two sets of drug peaks in the paracetamol ^{1}H NMR represented simultaneous binding of two CB[7] molecules to the drug.

2.3 X-Ray crystal structure of memantine and CB[7]

Crystals of the host–guest complex of memantine hydrochloride and CB[7] suitable for X-ray structure analysis were obtained from the slow evaporation of an equimolar solution of memantine hydrochloride and CB[7] in water (Table 2). Each of the two crystallographically independent host–guest complexes crystallise with 10 water molecules and a chloride counter ion. Both the counter ions and the solvent molecules are disordered, the latter over 51 separate sites. Memantine is almost totally bound inside the CB[7] cavity, with the binding stabilised by two hydrogen bonds (1.95 and 2.21 Å) from the memantine amine group to two separate oxygens of CB[7] (Fig. 6).

2.4 Molecular modelling

Using the ^{1}H NMR data, molecular models of atenolol, glibenclamide and paracetamol bound by CB[7] were generated. Minimised structures of atenolol and glibenclamide show hydrogen

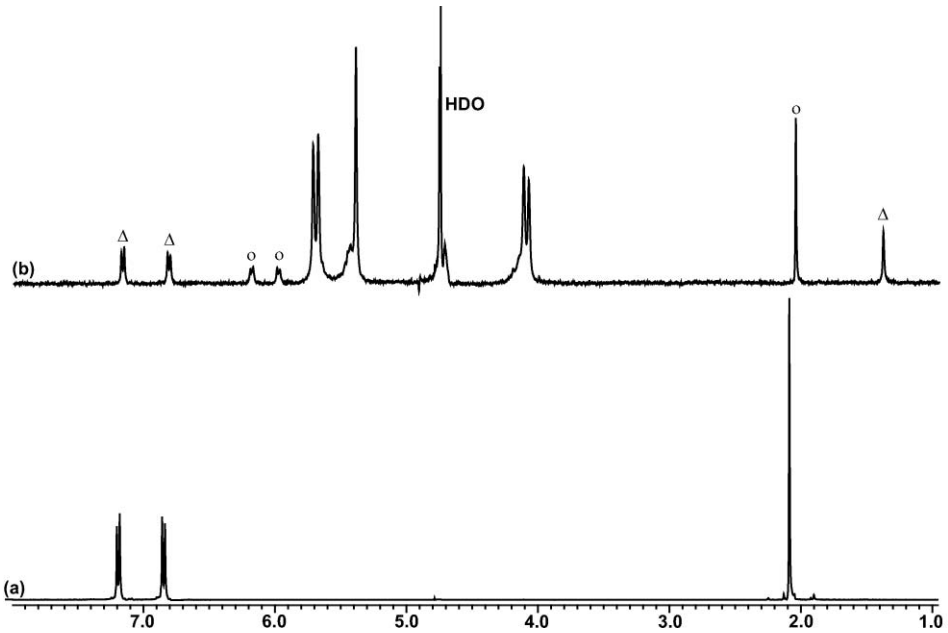

Fig. 5 The ^{1}H NMR spectra (D_2O) of (a) free paracetamol and (b) paracetamol with excess CB[7]. The two sets of drug peaks indicates that CB[7] binds over the phenyl group (○) and the methyl group (△) simultaneously, with the macrocycle shuttling between the two sites; see Fig. 8 for the proposed structures.

Table 2 Single crystal X-ray diffraction data for the host–guest complex of memantine hydrochloride and CB[7]

Dimension	Value
Empirical formula	$C_{54}H_{84.14}ClN_{29}O_{24.07}$
Formula weight	1560.26 g mol^{-1}
Crystal system	Monoclinic
Space group	$P2_1/n$
Unit cell dimensions	
a	21.273(10) Å
b	17.264(9) Å
c	38.427(19) Å
α, β, γ angles	90, 101.735(7), 90°
Volume	13 818(12) Å^3
Z	8
Density	1.500 Mg m^{-3}
Crystal size	0.07 × 0.03 × 0.004 mm

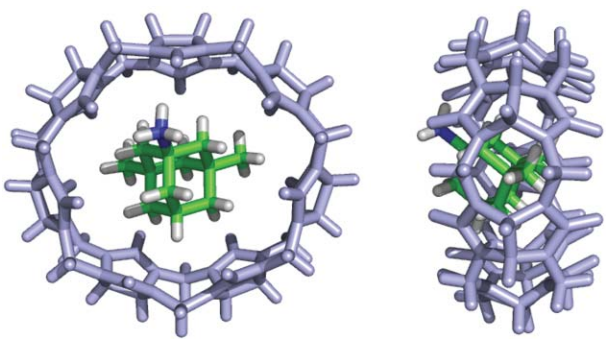

Fig. 6 The single crystal X-ray diffraction structure of the host–guest complex of memantine hydrochloride and CB[7]. For clarity, the chloride counter ion and waters of hydration have been omitted.

bonds between the drugs and CB[7]. Two hydrogen bonds are formed between the atenolol –OH and –NH_2 groups to the carbonyls of CB[7] on opposite sides of the macrocycle (Fig. 7). Comparatively, glibenclamide also forms two hydrogen bonds, although both are from the sulfonamide-NH group, to two adjacent carbonyls on one side of CB[7] (see Fig. 7).

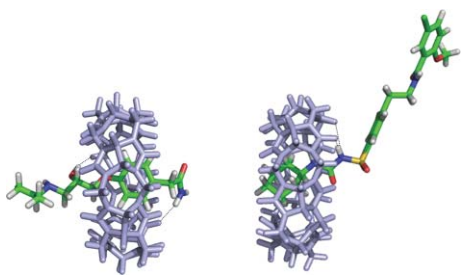

Fig. 7 Minimised host–guest structures of atenolol (left) and glibenclamide (right) with CB[7] (blue). Intermolecular hydrogen bonds are shown as dotted lines.

In generating molecular models for paracetamol, two different techniques were used. The first involved static models, where the drug was placed within the cavity in the approximate positions indicated by the ^{1}H NMR, then the host–guest complex was energy minimised. In the second, a single paracetamol molecule was pulled through the centre of CB[7], by making it travel towards a fixed methane molecule on the other side of the macrocycle, with the total system energy measured at regular specific time intervals (Fig. 8a and 8b, and ESI†). From this, global and local energy minima could be observed. Interestingly, the two paracetamol structures obtained have either one (–NH amide to imidazolidinone oxygen when the methyl group is within the cavity) or two (hydroxyl and –NH amide to imidazolidinone oxygens on opposite sides of CB[7] when the phenyl ring is included) hydrogen bonds (Fig. 8a and 8b). This might explain

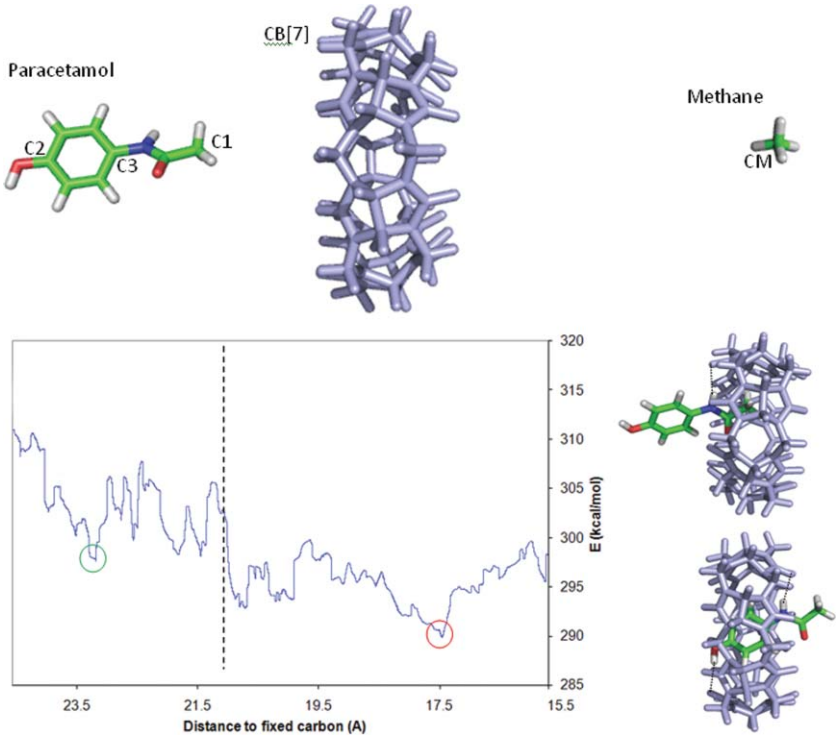

Fig. 8 **a.** Starting coordinates of paracetamol, CB[7] and methane prior to dynamics showing the alignment of CM, C1 and C2. **b.** Energy *versus* distance of C3 to CM for the minimised trajectory of paracetamol travelling through CB[7]. The vertical dotted line marks the transition when the phenyl ring of paracetamol starts entering the cavity of CB[7]. The minima for each region are circled in green (methyl of paracetamol within the cavity, picture top-right) and in red (phenyl of paracetamol within the cavity, picture bottom-right). Intermolecular hydrogen bonds are shown as dotted lines.

how shuttling between the two sites occurs; whilst the drug is hydrogen bonded twice to the cucurbituril, loss of the hydroxyl hydrogen bond leads to slipping through the cavity, but as the molecule is about to escape with its methyl group still included within the cavity, a hydrogen bond is formed again with the amide –NH group. When this hydrogen bond breaks, the drug can either become free, or slide back onto the phenyl group to form two hydrogen bonds again.

2.5 Determination of binding constants

Unfortunately, neither paracetamol, glibenclamide nor atenolol are fluorescent, and when CB[7] is titrated into solutions of these drugs there is no significant change in their UV absorbance. As such, binding constants were determined using a fluorescence displacement assay based on 2-aminoanthracene (2-AAH) at pH 1.5, for which a binding constant of 8×10^5 M^{-1} has previously been reported.[40] This pH is similar to that found in the stomach and, as such, is directly relevant to studying orally delivered drugs. In the absence of CB[7], 2-AAH fluoresces strongly at 508 nm, but when bound by CB[7] fluorescence at this wavelength decreases significantly, and instead it fluoresces at 388 and 410 nm (Fig. 9a).[40]

Titration of atenolol or glibenclamide into a 1 : 1 solution of 2-AAH and CB[7] (5 μM) increases the fluorescence of 2-AAH at 508 nm, and generates binding curves from which the binding constants of both drugs can be determined (Fig. 9b): atenolol, 4.2×10^4 M^{-1} and glibenclamide, 1.7×10^5 M^{-1}. Titration with paracetamol does not significantly change the fluorescence of 2-AAH. Subsequent examination of the paracetamol and CB[7] at

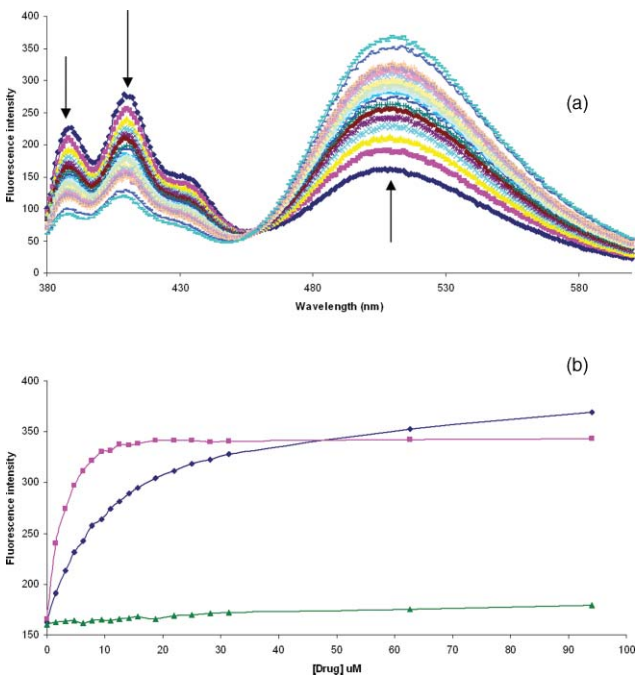

Fig. 9 **a.** The change in fluorescence of 2-aminoanthracene (5 μM) in the presence of an equimolar concentration of CB[7] at pH 1.5, upon titration of atenolol into the solution. The arrows indicate the direction of change. **b.** Binding curves of glibenclamide (pink), atenolol (blue) and paracetamol (green) generated from the increase in fluorescence of 2-aminoanthracene at 508 nm, using a fluorescence guest displacement assay.

pH 1.5 in DCl/D_2O by ^1H NMR shows that the drug does not form a host–guest complex at this pH, and therefore no binding constant could be determined.

2.6 Differential scanning calorimetry

Drug stability is important in the manufacture of drugs both in terms of processing and formulation.[41] Drug degradation into ineffective or harmful by-products reduces shelf life, and poor polymorphic physical stability can affect efficacy, safety, manufacturing reproducibility and cost. For instance, a change from an amorphous to crystalline structure, from one crystal polymorph to another, or dehydration/hydration of the solid can affect the drug's delivered dose, solubility and rate of dissolution, and through that, bioavailability and efficacy.[42] These changes can also affect the drug in automated manufacturing, for instance flow rates through hoppers and dyes, as well as tablet compaction and robustness.

Changes in macromolecular structure are particularly relevant for the four drugs studied here. Paracetamol is known to exist in three different crystal polymorphs, including a stable polymorph I and metastable polymorph II, the latter of which dissolves faster in water and is used in tablets.[43] With heating, polymorph II can be converted into the less desirable polymorph I. Glibenclamide is known to form irregular and asymmetrically structured crystals when cooled quickly from various solvents, but when cooled quickly after melting, it forms an amorphous solid with considerably different water solubility.[44] Memantine, whilst a simple small organic drug, can be produced as an amorphous powder,[45] in different crystal polymorphs[46] or even as a monohydrate.[47] Atenolol has one chiral centre, either *R* or *S*, which greatly affects its biological activity.[48] Crystals grown from either a racemic mixture of *R* and *S*, or from a pure *S*-form produce a hydrogen-bonded network of drugs with differing conformations[49] and, therefore, possibly different macromolecule properties for drug delivery. Given that drug manufacture, processing and formulation can expose drugs to temperatures of up to 80 °C with 100% relative humidity for periods of up to 6 h,[42] any one of the phase conversions for these four drugs can occur, greatly affecting the final product. It was therefore of interest to determine the effect of CB[7] on the physical stability of the four drugs examined in this study.

Each drug shows DSC curves (*e.g.* Fig. 10), melting points and enthalpies of fusion consistent with literature values:[43,44,50] glibenclamide (173.5–179.9 °C; –51.80 kJ mol^{-1}), paracetamol (168.6–174.1 °C; 29.19 kJ mol^{-1}) and atenolol (153.3–156.9 °C; –40.72 kJ mol^{-1}). Anhydrous memantine could not be analysed by DSC, so it was examined using scanning differential thermogravimetric analysis and shows a broad melting curve between 272 and 319 °C.

Addition of CB[7] has a significant effect on each drug. None of the three drugs melt below 280 °C under DSC conditions (and not below 380 °C for memantine), with the only effect seen being water loss at temperatures between 40 and 120 °C, which is similar to that seen for free CB[7] (Fig. 9). These results indicate that inclusion within CB[7] imparts significant physical stability on these drugs and may have applications in preventing drug degradation during manufacturing and storage, preventing interconversion between drug polymorphs, allowing production of a single form of a drug

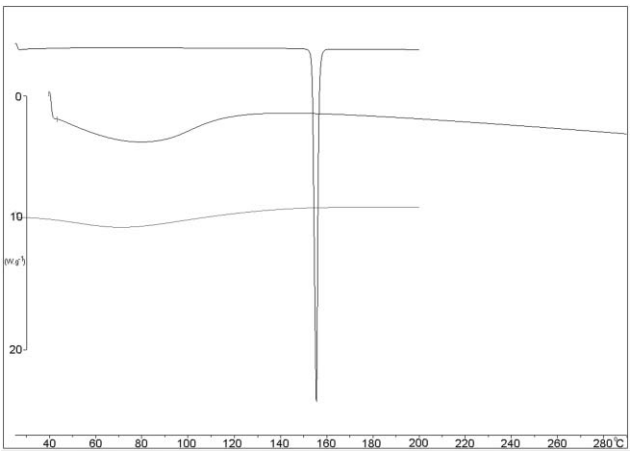

Fig. 10 The differential scanning calorimetry curves of (top) atenolol, (middle) CB[7] and (bottom) atenolol with 1 equivalent of CB[7], which is indicative of the curves also observed for glibenclamide, memantine and paracetamol.

which can be easier and/or cheaper than current methods, and allowing the use of prolonged or elevated temperatures during processing.

3. Conclusions

In this paper, we examined the host–guest chemistry of four orally active drugs with cucurbit[7]uril. Memantine is totally included within CB[7], atenolol is bound over the central part of the drug, glibenclamide is bound only over one end and paracetamol is bound in two different locations with the CB[7] shuttling between the two sites. As well as an increase in the water solubility of glibenclamide upon CB[7] binding, inclusion of each drug by CB[7] also imparts significant physical stability, which may have applications in the processing, manufacture and storage of organic drugs, as well as in drug delivery. These results now provide a chemical foundation to examining the use of CB[7]–drug host–guest complexes in oral tablet formulations, which we hope to report in the near future.

4. Experimental

4.1 Materials

Atenolol, glibenclamide, memantine, paracetamol and ibuprofen were purchased from Sigma-Aldrich. D_2O (99.9%) and d_6-DMSO (99.9%) were purchased from Cambridge Isotope Laboratories. Cucurbit[7]uril was made as previously described.[51]

4.2 NMR

Stock solutions of CB[7] were made in D_2O to a concentration of 2 mM. Stocks of each drug (20 mM) were prepared in D_2O for atenolol, memantine and paracetamol and in d_6-DMSO for glibenclamide. Aliquots of CB[7] and drug were combined, and made up to 600 μL to yield various CB[7] : drug ratios with final concentrations between 0.5 and 1.5 mM. ^1H NMR spectra were then recorded on a JOEL JNM-LA400 spectrometer. Spectra were obtained using between 16–128 scans, with a *d*1 of 2 s and a spectral width of 5000 Hz. Spectra were referenced internally to

the water peak for D_2O and to the methyl resonances of DSS in DMSO/D_2O mixed solvents.

4.3 ESI-MS

Positive ion electrospray ionisation (ESI) mass spectra were recorded on a Finnigan LTQ Orbitrap. Samples were dissolved in H_2O to a concentration of 500 μM, then 40 μL was diluted to 1 mL with a 50% methanol–50% 0.1 M formic acid solution and injected into the instrument at a flow rate of 400 μL min^{-1}. The capillary temperature and voltage were 230 °C and 40 V, respectively, with a source voltage of 4500 V.

4.4 X-Ray crystal structure

Crystal data for the host–guest complex of memantine hydrochloride and CB[7]: $C_{54}H_{84.14}Cl_1N_{29}O_{24.07}$, M_r = 1560.26. The structure was solved using SIR2004[52] and refined with SHELXL-97.[53] Data were measured at Station 19 of the DIAMOND synchrotron radiation source with a wavelength of 0.68890 Å to give: monoclinic, space group $P2_1/n$, a = 21.273(10), b = 17.264(9), c = 38.427(19) Å, β = 101.735(7)°, V = 13 818(12) Å^3, Z = 8, λ = 0.6566 Å, μ = 0.156 mm^{-1}, T = 120 K; 96 875 reflections, 20 850 unique, R_{int} 0.0856; final refinement to convergence on F^2 and with 2070 refined parameters gave R = 0.0793 (F, 13 159 obs. data only) and R_w = 0.2513 (F^2, all data), GOF = 1.043. CCDC reference numbers 746893. See the ESI for crystallographic data in CIF or other electronic format.†

4.5 Molecular modelling

Insight II and CDiscover software (Accelrys Inc., San Diego, CA) were used to perform all calculations and molecule handling employing the cff force field (for both atom typing and charges). All simulations were performed using a dual processor Hewlett-Packard 3.2 GHz xw8200 workstation. The starting cucurbit[7]uril structure was obtained from a single-crystal X-ray structure[54] and the drugs atenolol, glibenclamide and paracetamol manually docked, placing the drug in a region corresponding to a high shielding of its protons, as determined by NMR (two starting structures for paracetamol). The systems were then allowed to minimise without restraints, thereby providing a model structure for observation. In the case of paracetamol, both starting structures converged to give the same final complex (with CB[7] encapsulating the central phenyl ring of the drug), and a steered dynamics simulation followed by restrained minimisation of each snapshot generated by the dynamics run was necessary to observe the other inclusion mode.

Simulations were performed *in vacuo* using a distance-dependent dielectric constant of $1r_{ij}$ (dynamics) or $4r_{ij}$ (minimisation). For the dynamics run, we modified methodologies previously developed to force a DNA intercalating ligand to rotate in the plane formed between two sets of base pairs[55] or to travel along the minor groove of DNA[56] to study the interactions between the ligand and the macromolecule. Here, we used a fixed dummy methane molecule, which was added 18 Å away from the centre of geometry of CB[7] whilst a paracetamol molecule was manually placed 9 Å away on the other side of CB[7] (Fig. 7a). The carbon of the methane (CM) was used as an anchor to steer the paracetamol through CB[7] with quadratic distance restraints applied between the paracetamol methyl carbon (C1) and CM (10 Å target, 0.01 kcal mol^{-1} force constant). Extra distance restraints (16.5 Å target, 10 kcal mol^{-1} force constant) had to be applied between the 7 carbonyl oxygens of CB[7] facing CM and CM itself to prevent the cucurbituril from tilting. Another set of distance restraints (2 Å target, 0.01 kcal mol^{-1} force constant) was applied between the same oxygens from CB[7] and both C1 and the carbon bonded to the hydroxyl group of paracetamol (C2) in an attempt to keep CM, C1 and C2 in alignment with each other. 10 ps of simulation were required for the drug to travel through CB[7] and a snapshot saved every 1 fs (saving 10 000 snapshots in total). Each pose was then energy minimised (until a derivative of 0.1 kcal mol^{-1} Å^{-2} was achieved), keeping the methane fixed, all the CB[7] atoms tethered (10 kcal mol^{-1} force constant) and the phenyl ring carbon attached to the nitrogen atom of paracetamol (C3) fixed. This latest constraint was necessary to avoid any translational movement from the paracetamol during minimisation so as to obtain an energy value for the system as the drug travelled through CB[7] (Fig. S1, a movie of the minimised trajectory is supplied in the ESI†).

4.6 Determination of binding constants

CB[7] and 2-AAH (5 μM) were dissolved in water (3.000 mL), which had previously been adjusted to pH 1.5 by the addition of HCl. Fluorescence intensity was determined on a Varian Cary Eclipse spectrophotometer in a 1 cm quartz cell, using an excitation wavelength of 374 nm, with a medium scan speed between 380 and 600 nm, under similar conditions to those used by Wang *et al.*[40] Atenolol, glibenclamide or paracetamol (2.5 mM) were then titrated into the solution in 2, 4 or 40 μL increments, with mixing of the solutions before fluorescence was measured. Binding constants were determined based on previous displacement assays using ethidium bromide[57,58] and the equation:

$$K_{2\text{-AAH}}[\text{2-AAH}] = K_C[\text{Drug}]$$

where $K_{2\text{-AAH}}$ is the binding constant of 2-AAH to CB[7] (8.0×10^5 M^{-1}),[40] [2-AAH] is the fixed concentration of 2-AAH, K_C is the binding constant of either atenolol or glibenclamide and [Drug] is the concentration of drug that gives a 50% increase in fluorescence at 508 nm.

4.7 SDTA and DSC

Experiments were conducted using a Mettler Toledo TGA/SDTA 851e and Mettler Toledo DSC 8222e. Each sample (approximately 2–10 mg), prepared by freeze drying a 1 : 1 CB[7] : drug solution from water–DMF, was placed in an alumina or sealed aluminium pan, and weighed. Samples were then heated at a rate of 10 °C min^{-1}.

Acknowledgements

X-Ray diffraction was completed by the EPSRC synchrotron National Crystallography Service based at the Universities of Newcastle and Southampton.

References

1 R. K. Verma, D. M. Krishna and S. Garg, *J. Controlled Release*, 2002, **79**, 7–27.

2 Y.-F. Huang, D. Shangguan, H. Liu, J. A. Phillips, X. Zhang, Y. Chen and W. Tan, *ChemBioChem*, 2009, **10**, 862–868.
3 C. Cortez, E. Tomaskovic-Crook, A. P. R. Johnston, A. M. Scott, E. C. Nice, J. K. Heath and F. Caruso, *ACS Nano*, 2007, **1**, 93–102.
4 S. Dhar, Z. Liu, J. Thomale, H. Dai and S. J. Lippard, *J. Am. Chem. Soc.*, 2008, **130**, 11467–11476.
5 S. Abdul and S. S. Poddar, *J. Controlled Release*, 2004, **97**, 393–405.
6 J. Lagona, P. Mukhopadhyay, S. Chakrabarti and L. Isaacs, *Angew. Chem., Int. Ed.*, 2005, **44**, 4844–4870.
7 L. Isaacs, *Chem. Commun.*, 2009, 619–629.
8 A. D. St-Jacques, I. W. Wyman and D. H. Macartney, *Chem. Commun.*, 2008, 4936–4938.
9 M. V. Rekharsky, T. Mori, C. Yang, Y. H. Ko, N. Selvapalam, H. Kim, D. Sobransingh, A. E. Kaifer, S. Liu, L. Isaacs, W. Chen, S. Moghaddam, M. K. Gilson, K. Kim and Y. Inoue, *Proc. Natl. Acad. Sci. U. S. A.*, 2007, **104**, 20737–20742.
10 R. Wang and D. H. Macartney, *Tetrahedron Lett.*, 2008, **49**, 311–314.
11 R. Wang, L. Yuan and D. H. Macartney, *Chem. Commun.*, 2006, 2908–2910.
12 S. Liu, A. D. Shukla, S. Gadde, B. D. Wagner, A. E. Kaifer and L. Isaacs, *Angew. Chem., Int. Ed.*, 2008, **47**, 2657–2660.
13 I. Osaka, M. Kondou, N. Selvapalam, S. Samal, K. Kim, M. V. Rekharsky, Y. Inoue and R. Arakawa, *J. Mass Spectrom.*, 2006, **41**, 202–207.
14 M. A. Rankin and B. D. Wagner, *Supramol. Chem.*, 2004, **16**, 513–519.
15 B. D. Wagner, P. G. Boland, J. Lagona and L. Isaacs, *J. Phys. Chem. B*, 2005, **109**, 7686–7691.
16 J. Lagona, B. D. Wagner and L. Isaacs, *J. Org. Chem.*, 2006, **71**, 1181–1190.
17 B. D. Wagner, N. Stojanovic, A. I. Day and R. J. Blanch, *J. Phys. Chem. B*, 2003, **107**, 10741–10746.
18 L. Leclercq, N. Noujeim, S. H. Sanon and A. R. Schmitzer, *J. Phys. Chem. B*, 2008, **112**, 14176–14184.
19 N. J. Wheate, P. G. A. Kumar, A. M. Torres, J. R. Aldrich-Wright and W. S. Price, *J. Phys. Chem. B*, 2008, **112**, 2311–2314.
20 S. Kemp, N. J. Wheate, S. Wang, J. G. Collins, S. F. Ralph, A. I. Day, V. J. Higgins and J. R. Aldrich-Wright, *JBIC, J. Biol. Inorg. Chem.*, 2007, **12**, 969–979.
21 V. Sindelar, S. E. Parker and A. E. Kaifer, *New J. Chem.*, 2007, **31**, 725–728.
22 A. Praetorius, D. M. Bailey, T. Schwarzlose and W. M. Nau, *Org. Lett.*, 2008, **10**, 4089–4092.
23 P. Montes-Navajas, L. Teruel, A. Corma and H. Garcia, *Chem.–Eur. J.*, 2008, **14**, 1762–1768.
24 J. Mohanty, A. Bhasikuttan, S. D. Choudhury and H. Pal, *J. Phys. Chem. B*, 2008, **112**, 10782–10785.
25 J. Choi, J. Kim, K. Kim, S.-T. Yang, J.-I. Kim and S. Jon, *Chem. Commun.*, 2007, 1151–1153.
26 K. M. Park, K. Suh, H. Jung, D.-W. Lee, Y. Ahn, J. Kim, K. Baek and K. Kim, *Chem. Commun.*, 2009, 71–73.
27 N. J. Wheate, *J. Inorg. Biochem.*, 2008, **102**, 2060–2066.
28 S. Kemp, N. J. Wheate, F. H. Stootman and J. R. Aldrich-Wright, *Supramol. Chem.*, 2007, **19**, 475–484.
29 R. Wang, B. C. MacGillivray and D. H. Macartney, *Dalton Trans.*, 2009, 3584–3589.
30 Y. Zhao, D. P. Buck, D. L. Morris, M. H. Pourgholami, A. I. Day and J. G. Collins, *Org. Biomol. Chem.*, 2008, **6**, 4509–4515.
31 S. Liu, C. Ruspic, P. Mukhopadhyay, S. Chakrabarti, P. Y. Zavalij and L. Isaacs, *J. Am. Chem. Soc.*, 2005, **127**, 15959–15967.
32 M. V. Rekharsky, H. Yamamura, Y. H. Ko, N. Selvapalam, K. Kim and Y. Inoue, *Chem. Commun.*, 2008, 2236–2238.
33 J. Kim, Y. Ahn, K. M. Park, Y. Kim, Y. H. Ko, D. H. Oh and K. Kim, *Angew. Chem., Int. Ed.*, 2007, **46**, 7393–7395.
34 I. Hwang, K. Baek, M. Jung, Y. Kim, K. M. Park, D.-W. Lee, N. Selvapalam and K. Kim, *J. Am. Chem. Soc.*, 2007, **129**, 4170–4171.
35 D. P. Buck, P. M. Abeysinghe, C. Cullinane, A. I. Day, J. G. Collins and M. M. Harding, *Dalton Trans.*, 2008, 2328–2334.
36 K. Uekama, F. Hirayama and H. Arima, *J. Inclusion Phenom. Macrocyclic Chem.*, 2006, **56**, 3–8.
37 K. Uekama, F. Hirayama and T. Irie, *Chem. Rev.*, 1998, **98**, 2045–2076.
38 R. Challa, A. Ahuja and R. K. Khar, *AAPS PharmSciTech*, 2005, **6**, E329–E357.
39 S. Walker, R. Kaur, F. J. McInnes, N. J. Wheate, Oral drug formulations, 2009, *UK patent application*, number GB0906003.9, 24 pp.
40 R. Wang, L. Yuan and D. H. Macartney, *Chem. Commun.*, 2005, 5867–5869.
41 J. T. Carstensen, *Drug stability: Principles and practices*, 2nd edn, 1995, vol. 68, Marcel Dekker Inc, New York.
42 H. G. Brittain, *Polymorphism in pharmaceutical solids*, 1999, vol. 95, Marcel Dekker Inc, New York.
43 E. V. Boldyreva, V. A. Drebushchak, I. E. Paukov, Y. A. Kovalevskaya and T. N. Drebushchak, *J. Therm. Anal. Calorim.*, 2004, **77**, 607–623.
44 G. G. G. Oliveira, H. G. Ferraz and J. S. R. Matos, *J. Therm. Anal. Calorim.*, 2005, **79**, 267–270.
45 L. Huang, Novel amorphous form of memantine hydrochloride, 2005, *US patent*, number 20050222271.
46 Merli V. D. Paola, Adrienne Kovacsne-Mezei, Judith Aronhime, Precipitation process for the preparation of polymorphic crystalline forms of memantine hydrochloride, 2006, *International patent*, number WO 2006/076560.
47 Memantine hydrochloride hydrate, *Research Disclosure*, 2006, **505**, 518–519.
48 A. A. Pearson, T. E. Gaffney, T. Walle and P. J. Privitera, *J. Pharmacol. Exp.*, 1989, **250**, 759–763.
49 R. A. Esteves de castro, J. Canotilho, R. M. Barbosa, M. R. Silva, A. M. Beja, J. A. Paixão and J. S. Redinha, *Cryst. Growth Des.*, 2007, **7**, 496–500.
50 R. N. Pereira, B. R. Valente, A. P. Cruz, T. Foppa, F. S. Murakami and M. A. S. Silva, *Lat. Am. J. Pharm.*, 2007, **26**, 382–386.
51 A. Day, A. P. Arnold, R. J. Blanch and B. Snushall, *J. Org. Chem.*, 2001, **66**, 8094–8100.
52 M. C. Burla, R. Caliandro, M. Camalli, B. Carrozzini, G. L. Cascarano, L. De Caro, C. Giacovazzo, G. Polidori and R. Spagna, *J. Appl. Crystallogr.*, 2005, **38**, 381.
53 G. M. Sheldrick, *Acta Crystallogr., Sect. A*, 2008, **64**, 112–122.
54 J. Kim, I. S. Jung, S. Y. Kim, E. Lee, J. K. Kang, S. Sakamoto, K. Yamaguchi and K. Kim, *J. Am. Chem. Soc.*, 2000, **122**, 540–541.
55 R. L. Clark, F. M. Deane, N. G. Anthony, B. F. Johnston, F.O. McCarthy and S. P. Mackay, *Bioorg. Med. Chem.*, 2007, **15**, 4741–4752.
56 N. G. Anthony, G. Huchet, B. F. Johnston, J. A. Parkinson, C. J. Suckling, R. D. Waigh and S. P. Mackay, *J. Chem. Inf. Model.*, 2005, **45**, 1896–1907.
57 D. Bartulewicz, K. Bielawski and A. Bielawska, *Arch. Pharm.*, 2002, **335**, 422–426.
58 M. Lee, A. L. Rhodes, M. D. Wyatt, M. D'Incalci, S. Forrow and J. A. Hartley, *J. Med. Chem.*, 1993, **36**, 863–870.